Interaction of molybdenum hexacarbonyl with metallic aluminum at high temperatures: Carbide and alloy formation

Y. Wang, F. Gao, W.T. Tysoe *

Department of Chemistry and Biochemistry, Laboratory for Surface Studies, University of Wisconsin–Milwaukee, 3210 N. Cramer Street, Milwaukee, WI 53211, USA

Abstract

The reaction of $Mo(CO)_6$ on aluminum films grown on a $Mo(1\,0\,0)$ substrate at 700 K is explored in ultrahigh vacuum using temperature-programmed desorption (TPD) and Auger and X-ray photoelectron (XPS) spectroscopies. Reaction with $Mo(CO)_6$ at 700 K results in some oxidation of the outer layer of the aluminum film, and the formation of a molybdenum carbide, which incorporates some oxygen. The carbide stoichiometry varies initially from approximately MoC for carbonyl reacting with the aluminum surface, to Mo_2C for thicker films. Heating this film to ∼1200 K results primarily in the desorption of carbon monoxide due to a reaction between the carbide and aluminum oxide. Metallic aluminum diffuses from the bulk of the film and some aluminum is found to desorb from the surface at ∼1270 K so that aluminum is retained on the surface due to the presence of the carbonyl-derived film. It is suggested that the aluminum can form an alloy with molybdenum at these higher temperatures.
© 2005 Elsevier B.V. All rights reserved.

Keywords: X-ray photoelectron spectroscopy; Temperature-programmed desorption; Auger spectroscopy; Chemisorption; Molybdenum hexacarbonyl; Aluminum thin films

1. Introduction

Catalysts formed by reacting molybdenum hexacarbonyl with high-surface area oxides are active for a number of reactions, including alkene hydrogenation and metathesis [1–4] and several studies have been carried out, primarily using infrared spectroscopy, to understand the nature of the catalytically active surface species [5–12]. Model catalysts, consisting of thin oxide films onto which metal nanoparticles have been evaporated have been extensively investigated to gain a deeper understanding of the role of particle size and morphology on the catalytic activity [13–16]. There are several advantages to this approach. First, the thin oxide film deposited onto a metal substrate allows electron-based spectroscopies to be used to interrogate the surface since the film is sufficiently thin that it does not charge [17–27]. In addition, other,

non-electron-based techniques, such as reflection–absorption infrared spectroscopy (RAIRS) can also be used. Second, it is relatively easy to modify the oxide, for example by isotopic labeling, by forming the oxide with $H_2{}^{18}O$ or D_2O. Finally, the activity of the model catalyst can be measured without intervening exposure to air by moving it from ultrahigh vacuum into a high-pressure reactor incorporated in an ultrahigh vacuum system. This also allows any changes caused by the catalytic reaction to be monitored merely by moving the sample back into ultrahigh vacuum.

The formation of model catalysts using metal carbonyls has several attractive advantages. First, it enables models to be prepared in a manner that more closely mimics that used to prepare high-surface area catalysts. Second, it potentially allows the formation of novel surface structures that would not otherwise be accessible by evaporating a metal onto the surface. The interaction between molybdenum hexacarbonyl and alumina thin films has been studied in ultrahigh vacuum (UHV) by us [28–31] and others [32]. $Mo(CO)_6$ desorbs

* Corresponding author. Tel.: +1 414 229 5222; fax: +1 414 229 5036.
  E-mail address: wtt@uwm.edu (W.T. Tysoe).

molecularly from the surface below ~250 K and also reacts to form strongly bound species, where these reaction pathways compete [28,30]. The CO from the strongly bound surface species desorbs in two states in temperature-programmed desorption (TPD) with a profile that is very similar to that found on high-surface-area substrates. This strongly bound species has been identified on aluminas with various degrees of hydroxylation as an oxalate species, which decomposes by desorbing CO at ~320 and 430 K [28,30,31]. Unfortunately, because of the kinetic competition between carbonyl desorption at ~250 K and decomposition to form the surface species, only relatively small molybdenum coverages (a few percent of a monolayer) can be achieved in ultrahigh vacuum. Recent theoretical calculations have emphasized the difficulties associated with $Mo(CO)_6$ dissociation on unreactive surfaces [33]. It has been shown that $Mo(CO)_6$ can be decarbonylated when illuminated with ultraviolet radiation [34–36] and also using electron beams [31]. The resulting surface species are relatively inactive in UHV. Complete decarbonylation of the carbonyl typically occurs at or below ~600 K [28–31,37]. It is therefore possible to deposit pure Mo particles on the surface at a substrate temperature higher than 600 K. However, since the resulting molybdenum easily dissociates CO, pure metal deposition is generally difficult. In fact, Burwell et al. have found that reaction of $Mo(CO)_6$ with dehydrogenated alumina in flowing helium produced a surface with a C/Mo ratio of 0.3/0.4 [38]. It has also been shown that molybdenum carbide is formed when $Mo(CO)_6$ is deposited onto thin alumina films at 700 K [29]. It has been found that the presence of surface hydroxyl groups on the alumina have a profound effect on the final oxidation state of Mo species during $Mo(CO)_6$ decarbonylation. Metallic molybdenum has been observed to form on fully dehydroxylated alumina [32] but has been demonstrated to be unstable in contact with OH groups on alumina at temperatures higher than 473 K [6].

Despite the extensive investigations of $Mo(CO)_6$ with alumina, to our knowledge, there have been no studies of the interaction of $Mo(CO)_6$ with metallic aluminum. As a precursor to studying the high-temperature decomposition of molybdenum carbonyl with alumina films in greater detail, the chemistry on metallic aluminum has been studied in the following.

2. Experimental

Temperature-programmed desorption (TPD) data were collected in an ultrahigh vacuum chamber operating at a base pressure of 8×10^{-11} Torr that has been described in detail elsewhere [38,39] where desorbing species were detected using a Dycor quadrupole mass spectrometer placed in line of sight of the sample. This chamber was also equipped with a double-pass cylindrical mirror analyzer for collecting Auger spectra.

X-ray photoelectron spectra (XPS) were collected in another chamber operating at a base pressure of 2×10^{-10} Torr, which was equipped with Specs X-ray source and double-pass cylindrical mirror analyzer. Spectra were typically collected with an Mg Kα X-ray power of 250 W and a pass energy of 50 eV. The deposited film was sufficiently thin that no charging effects were noted and the binding energies were calibrated using the Mo $3d_{5/2}$ feature (at 227.4 eV binding energy) as a standard.

Temperature-programmed desorption spectra were collected at a heating rate of 15 K/s. Temperature-dependent XP and Auger spectra were collected by heating the sample to the indicated temperature for 5 s, allowing the sample to cool to 300 K, following which the spectrum was recorded.

The Mo(1 0 0) substrate (1 cm diameter, 0.2 mm thick) was cleaned using a standard procedure, which consisted of argon ion bombardment (2 kV, 1 μA/cm^2) and any residual contaminants were removed by briefly heating to 2000 K in vacuo. The resulting Auger spectrum showed no contaminants. Aluminum was deposited onto Mo(1 0 0) from a small heated alumina tube, which was enclosed in a stainless-steel shroud to minimize contamination of other parts of the system [40].

Molybdenum hexacarbonyl (Aldrich, 99%) was transferred to a glass vial, connected to the gas-handling line of the chamber and purified by repeated freeze–pump–thaw cycles, followed by distillation, and its purity was monitored using mass and infrared spectroscopies. This was also dosed onto the surface via a capillary doser to minimize background contamination. The exposures in Langmuirs (1 L = 1 × 10^{-6} Torr s) are corrected using an enhancement factor determined using temperature-programmed desorption (see [28] for a more detailed description of this procedure).

3. Results

Fig. 1a shows a series of Auger spectra of $Mo(CO)_6$ adsorbed at 700 K onto a thin aluminum film deposited onto a Mo(1 0 0) substrate. $Mo(CO)_6$ exposures are marked adjacent to each spectrum. Shown for comparison is the spectrum of the film prior to any carbonyl adsorption. Aluminum is deposited onto the Mo(1 0 0) single crystal held at room temperature where the thickness of the aluminum film is adjusted to be sufficient to suppress the substrate molybdenum Auger signals ensuring that any molybdenum detected following $Mo(CO)_6$ adsorption derives from the carbonyl. Kinetic energies were calibrated using the substrate Mo MNV transition [41,42] at 186 eV as the standard.

The freshly deposited aluminum film has a LVV Auger transition at 65.4 eV kinetic energy and assigned to metallic aluminum. Note that a small aluminum feature at ~54 eV and an oxygen signal at ~510 eV are also observed. This indicates that a portion of the aluminum has oxidized during deposition and XPS analyses (see below) indicate the presence of both Al^0 and Al^{3+} in the aluminum film immediately following deposition.
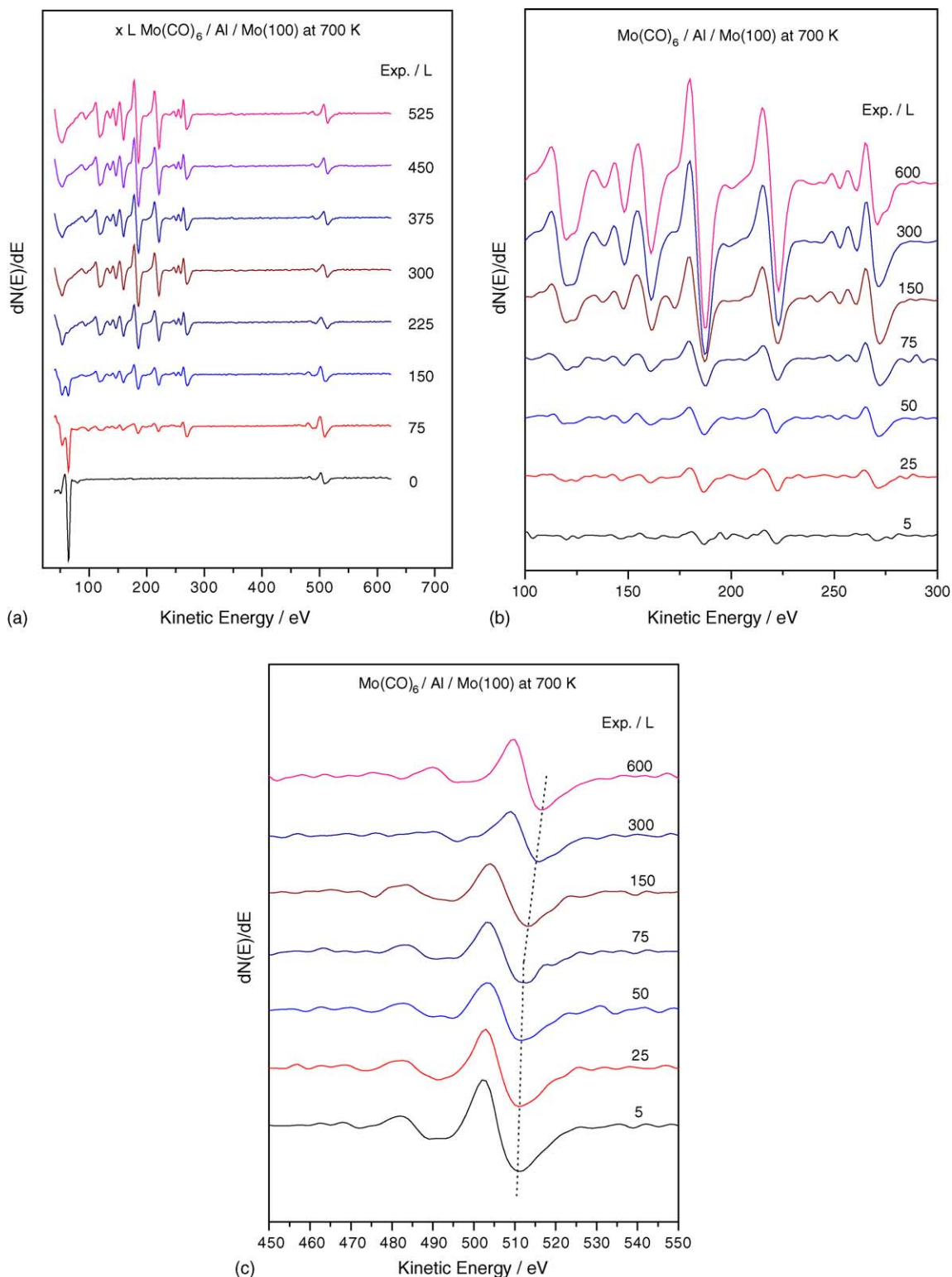
Fig. 1. Auger spectra of molybdenum hexacarbonyl deposited onto thin aluminum films grown on a Mo(1 0 0) substrate at a sample temperature of 700 K: (a) wide scan spectrum collected as a function of Mo(CO)$_6$ exposure, (b) a narrow scan spectrum between 100 and 300 eV kinetic energy collected as a function of Mo(CO)$_6$ exposure showing the molybdenum and carbon Auger transitions, and (c) a narrow scan spectrum between 450 and 550 eV kinetic energy showing the O KLL peak, all collected as a function of Mo(CO)$_6$ exposure. In all cases, exposures are marked adjacent to the corresponding spectrum.

Fig. 1a shows that the aluminum is oxidized with increasing Mo(CO)$_6$ exposure where oxidation of the outermost aluminum layers (within the probe depth of Auger spectroscopy ~10 Å) is complete following a Mo(CO)$_6$ exposure of ~300 L. This oxidation is presumably caused by oxygen resulting from CO released by Mo(CO)$_6$ decarbonylation. Blank experiments carried out by dosing CO onto the freshly deposited aluminum film at 700 K do not oxidize the aluminum, so that CO dissociation appears to be induced by molybdenum. Fig. 1b reveals that both molybdenum (from the features at 119, 160, 186 and 221 eV kinetic energy) and carbon (from the feature at 281 eV kinetic energy) are deposited onto the surface. The intensity of the molybdenum and carbon Auger features increases as a function of exposure and saturates at an exposure of between 300 and 600 L. The characteristic shape of carbon KLL transition indicates that the carbon is present as carbide [29]. The expanded spectrum of Fig. 1c reveals a shift in the oxygen KLL Auger transition from 510 to 514.5 eV with increasing Mo(CO)$_6$ exposure. This effect will be discussed below in greater detail together with XPS data.

Fig. 2a shows Auger spectra of the film exposed to 525 L of Mo(CO)$_6$ at 700 K then briefly annealed to various temperatures. In this case, the sample was heated to the indicated temperature for 5 s and allowed to cool to room temperature, following which the Auger spectrum was collected. No significant spectral changes are found after annealing at 800 K. However, heating to 900 K results in the appearance of an intense metallic aluminum feature at ~65 eV kinetic energy. This process is also accompanied by a decrease in the molybdenum and oxygen Auger signal intensities. The intensity of the 65 eV metallic aluminum Auger signal increases and reaches a maximum after heating to 1000 K and starts to decrease at higher temperatures (Fig. 2b).

Fig. 3 presents temperature-programmed desorption data for various exposures of Mo(CO)$_6$ deposited on an aluminum film at 700 K and then heated to 1400 K at a heating rate of ~15 K/s. In all cases, very little CO$_2$, oxygen or Mo(CO)$_6$ is found to desorb and significant intensity is detected only at 27 and 28 amu. Note that the 28 amu traces have been attenuated by a factor of 10 so that a portion of the 27 amu signal is due to cross talk from the intense signal at 28 amu. For a Mo(CO)$_6$ exposure of 75 L (Fig. 3a), an intense 28 amu feature, due to CO desorption, is present with a peak temperature of ~1040 K. Also evident is a sharp additional feature at 1270 K in the 27 amu spectrum assigned to some aluminum desorbing from the surface. This temperature corresponds to that at which the aluminum Auger signal is observed to decrease in intensity (Fig. 2a), in accord with the observed aluminum desorption. As the Mo(CO)$_6$ exposure increases to 300 L (Fig. 3b) and 525 L (Fig. 3c), the intensity of the CO desorption state increases and the peak shifts slightly to lower temperatures. In addition, the 27 amu signal intensity decreases indicating that the amount of aluminum that desorbs from the surface
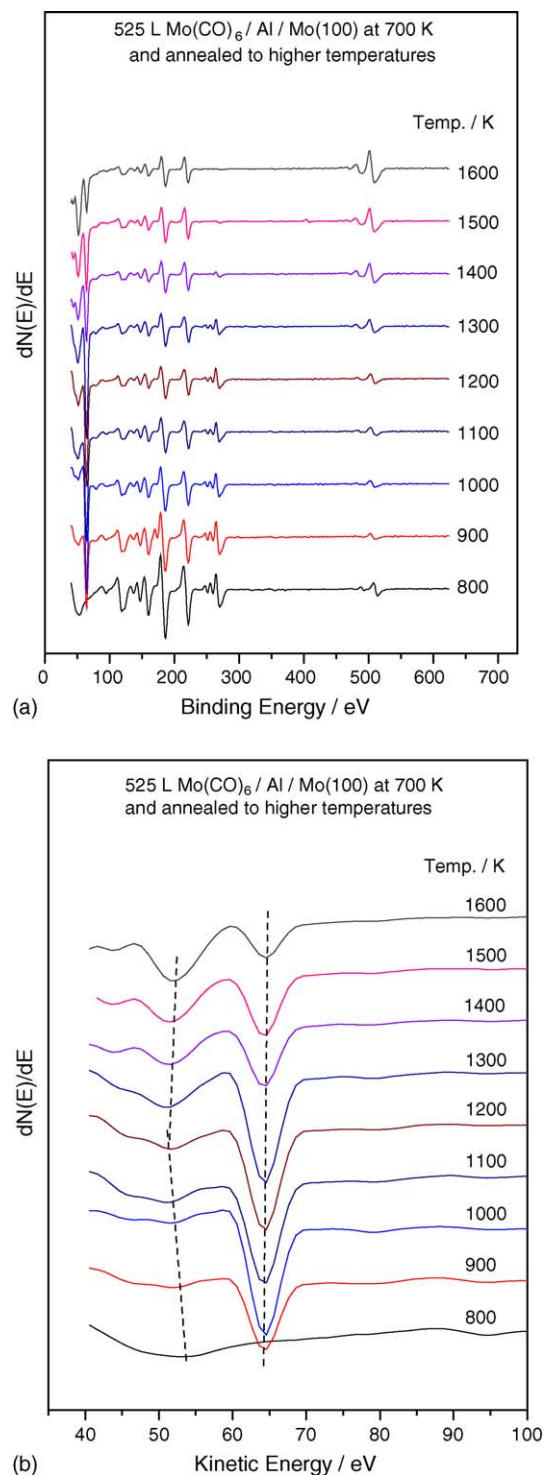
Fig. 2. Auger spectra of 525 L of Mo(CO)$_6$ deposited onto a thin aluminum film at 700 K and annealed to various temperatures, where the annealing temperatures are marked adjacent to the corresponding spectrum: (a) wide scan and (b) narrow scan between 40 and 100 eV kinetic energy showing the evolution of the Al LVV transition.
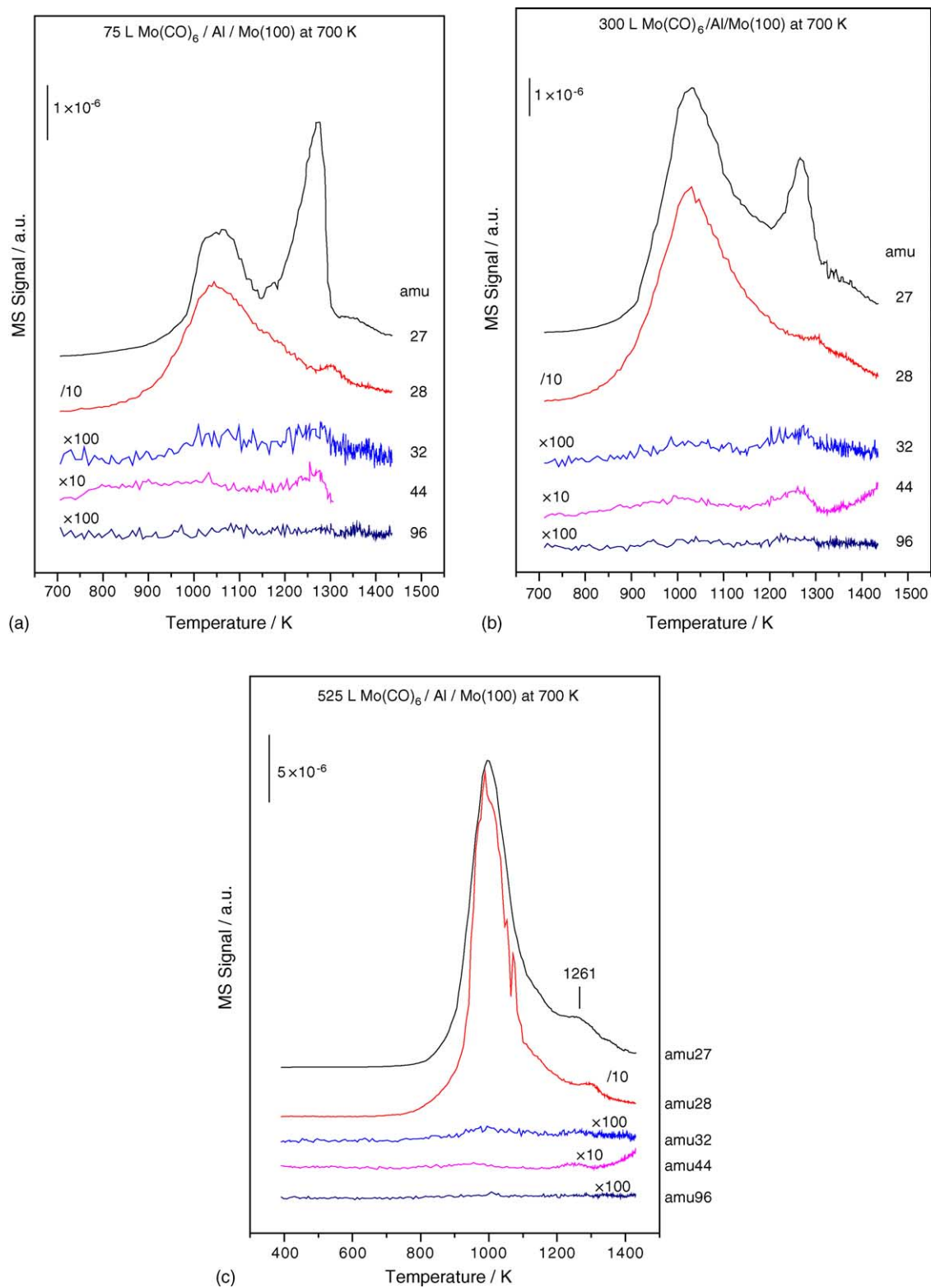
Fig. 3. Temperature-programmed desorption spectra collected at a heating rate of 15 K/s following the adsorption of $Mo(CO)_6$ on a thin aluminum film at 700 K. The $Mo(CO)_6$ exposures are: (a) 75 L, (b) 300 L and (c) 525 L, monitoring 96 amu ($Mo(CO)_6$), 44 amu (CO_2), 32 amu (O_2), 28 amu (CO) and 27 amu (Al).

also decreases. However, even at a $Mo(CO)_6$ exposure of 525 L (where no Al^0 is detected by AES), aluminum desorption at ~1260 K is still detectable. The intensity, however, is less than half of the aluminum desorption peak shown in Fig. 3a.

Fig. 4a displays the XPS spectra of $Mo(CO)_6$ deposited at 700 K onto a thin aluminum film grown on Mo(1 0 0), where again the aluminum film thickness was selected to be sufficiently large to suppress signals from the molybdenum substrate. In accord with the Auger results (Fig. 1), the feature at ~530 eV binding energy indicates that the freshly deposited aluminum film contains some oxygen. The peaks at 74 and 120 eV binding energy indicate the presence of aluminum on the surface. Exposure of the aluminum film to $Mo(CO)_6$ at 700 K results in the appearance of features at ~226 and 380 eV due to molybdenum and a feature at ~280 eV due to carbon [41]. Fig. 4b plots the integrated intensity of the Mo $3d_{5/2}$ XPS signal as a function of $Mo(CO)_6$ exposure. This shows no variation after a carbonyl exposure of ~500 L indicating that the film thickness at this point is greater than the photoelectron escape depth. This exposure is larger than that found when analyzing the film with Auger spectroscopy (Fig. 1) since the sampling depth of Auger spectroscopy is somewhat lower than that for XPS [42].

Fig. 5 shows narrow scans for the (a) Al 2p, (b) C 1s, (c) Mo 3d, and (d) O 1s regions. The Al 2p features Fig. 5a are distinguished by fitting with Gaussians. This reveals the presence of two components due to Al^0 at 72.0 eV binding energy and at 74.5 eV due to Al^{3+}. Evidently the freshly deposited aluminum films contain a small portion of Al^{3+}, consistent with the Auger measurements (Fig. 1a). Depositing $Mo(CO)_6$ on the surface at 700 K causes two clear changes: (1) the oxidation of metallic aluminum, and (2) a decrease in intensity of the Al 2p signal so that, following a 700 L $Mo(CO)_6$ dose at 700 K, only Al^{3+} is detected. Note that this does not necessarily mean that the aluminum film is completely oxidized as indicated by TPD results shown in Fig. 3.

Fig. 5b displays the corresponding C 1s feature, which increases in intensity with increasing $Mo(CO)_6$ exposure and the profiles are fit using a combined Gaussian/Lorentzian function. Prior to $Mo(CO)_6$ exposure, two types of carbon are detected with components at 284.4 and 281.8 eV binding energy. These are assigned to the presence of graphite and carbide impurities, respectively, deposited on the surface during aluminum film deposition. An additional feature grows with increasing $Mo(CO)_6$ exposure, becoming prominent for exposures greater than 100 L with a binding energy of 282.2 eV. This is assigned to the presence of carbide in accord with the C KLL Auger lineshape (Fig. 1). Note that this binding energy is different from that due to carbide initially present on the aluminum (at 281.8 eV binding energy), and is assigned to the formation of molybdenum carbide. Edamoto et al. recently studied the oxidation of Mo_2C by XPS [43] and discovered that molybdenum carbide oxidation induced a shoulder at a higher binding energy than the C 1s feature (283.5–284 eV). The data of Fig. 5b has no features at this

(a)

(b)
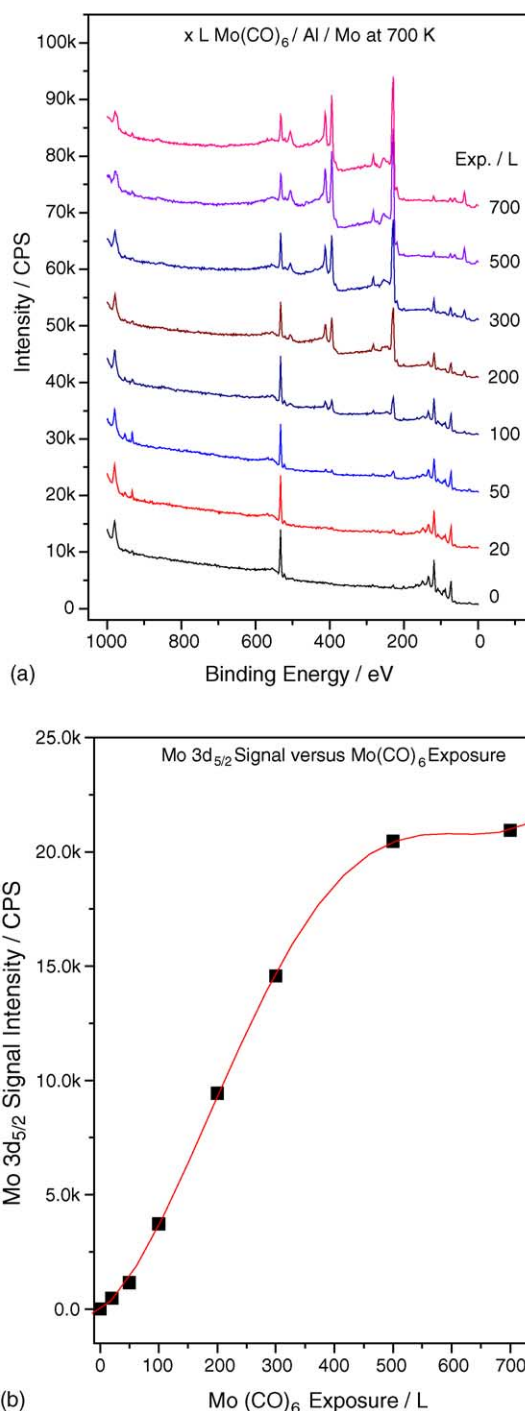
Fig. 4. (a) Mg $K\alpha$ X-ray photoelectron spectra of $Mo(CO)_6$ deposited onto a thin aluminum film on Mo(1 0 0) at 700 K as a function of $Mo(CO)_6$ exposure, where the exposures are marked adjacent to the corresponding spectrum. (b) A plot of the integrated intensity of the Mo $3d_{5/2}$ XPS signal as a function of $Mo(CO)_6$ exposure.

binding energy suggesting little oxidation of the carbidic carbon in this case.

Fig. 5c shows the corresponding Mo 3d features. A very small molybdenum signal is detected before $Mo(CO)_6$ exposure due to the molybdenum substrate at 227.3 eV binding
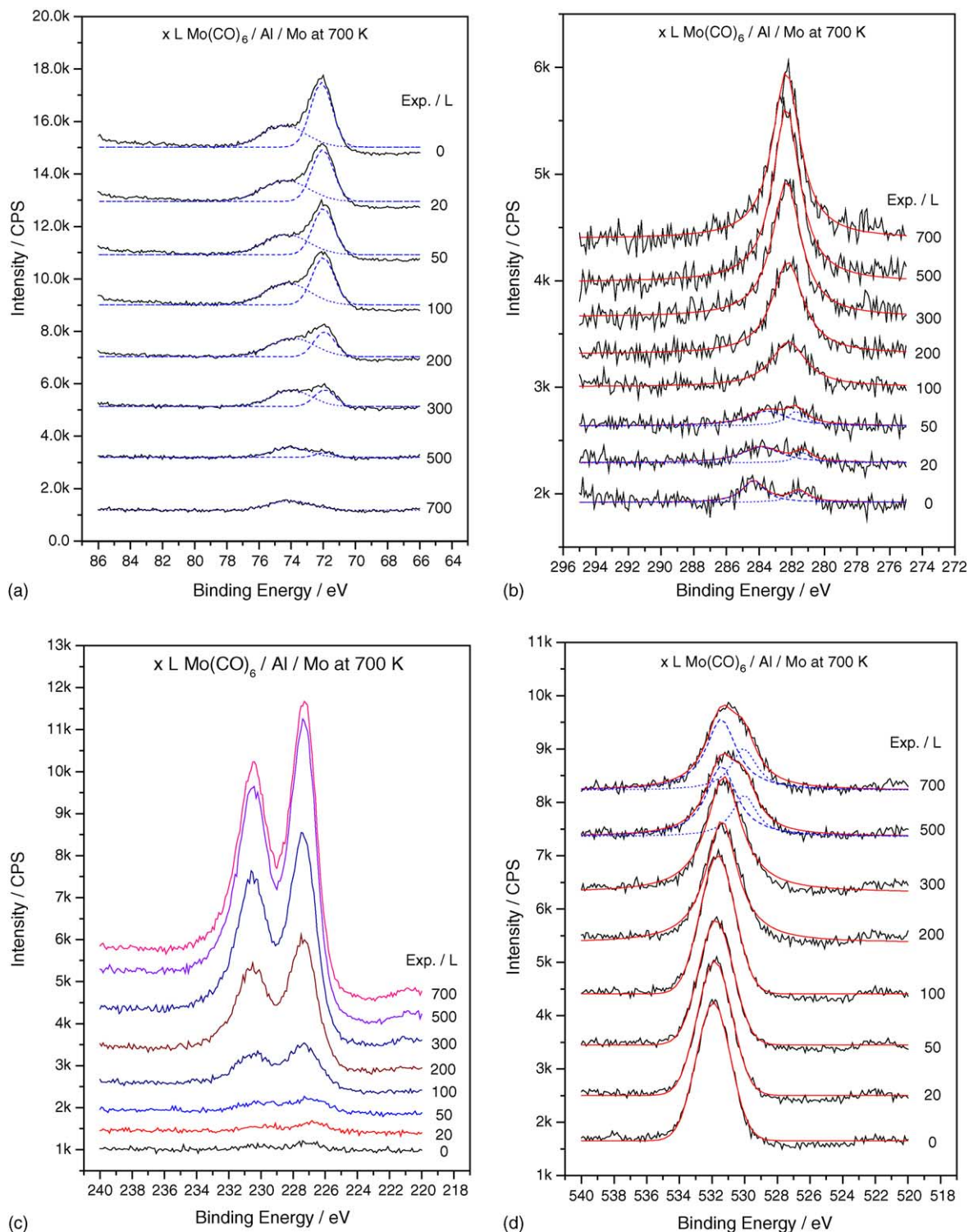
Fig. 5. Narrow scan Mg Kα X-ray photoelectron spectra of Mo(CO)$_6$ deposited onto a thin aluminum film on Mo(1 0 0) at 700 K as a function of Mo(CO)$_6$ exposure, where the exposures are marked adjacent to the corresponding spectra: (a) Al 2p, (b) C 1s, (c) Mo 3d and (d) O 1s regions.

energy, typical for metallic molybdenum [41]. When 20 L Mo(CO)$_6$ is deposited onto aluminum, the corresponding Mo 3d$_{5/2}$ binding energy shifts to 226.8 eV. As the Mo(CO)$_6$ exposure exceeds 50 L, the Mo 3d$_{5/2}$ binding energy returns to 227.3 eV indicative of the presence of molybdenum metal.

Shown in Fig. 5d is the corresponding O 1s spectral region as a function of carbonyl exposure. The film initially exhibits an O 1s feature at 531.9 eV binding energy, in accord with the Auger spectrum of the clean surface (Fig. 1). For Mo(CO)$_6$ exposures below 100 L, essentially
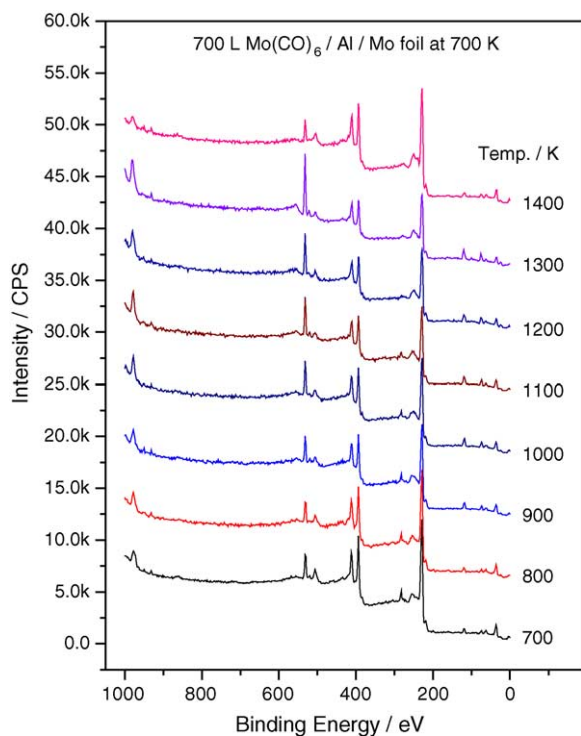
Fig. 6. Mg Kα X-ray photoelectron spectra of 700 L of Mo(CO)$_6$ deposited onto a thin aluminum film on Mo(1 0 0) at 700 K as a function of annealing temperature, where the annealing temperatures are marked adjacent to the corresponding spectrum.

no change in the oxygen spectrum is observed. However, for Mo(CO)$_6$ exposures of 200 L or higher, the O 1s binding energy decreases. In particular, for exposures greater than 300 L, an additional component appears at ~530 eV binding energy. An O 1s binding energy of ~530 eV was found for chemisorbed oxygen on a Mo(1 1 2) surface [44]. The spectra obtained using 500 and 700 L of Mo(CO)$_6$ were fit to two peaks (with components centered at 531.5 and 530.0 eV binding energy). This clearly indicates that a portion of the oxygen bonds to molybdenum. The oxygen KLL Auger transition shifts from 510 to 514 eV (Fig. 1c), which may indicate the interaction of oxygen with molybdenum.

The effect of annealing a surface formed by exposing aluminum to 700 L of Mo(CO)$_6$ at 700–1400 K is shown in the XPS data of Figs. 6 and 7. Fig. 7a shows the Al 2p features where no change is observed after annealing to 800 K. However, when the sample is annealed to 900 K, a metallic aluminum signal appears at ~72 eV, consistent with the Auger measurements shown in Fig. 2. This is proposed to be aluminum that diffuses from deep within the sample and this will be discussed in greater detail below. Drastic changes occur on heating to between 1100 and 1300 K. First, a feature grows at ~75.3 eV probably signifying that some Al^{3+} has been reduced to Al$^{\delta+}$ and second, the Al^0 feature at ~72 eV shifts to ~71.2 eV. Finally on heating to between 1300 and 1400 K, the binding energies of the aluminum fea-

tures do not vary but the intensity of Al$^{\delta+}$ signal decreases drastically.

Fig. 7b displays the Mo 3d spectra where, between 700 and 1100 K, the Mo signal intensity decreases slightly but shows no change in binding energy. On heating from 1100 to 1200 K, the Mo 3d$_{5/2}$ feature shifts from 227.2 to 226.7 eV. Since molybdenum is in its zero oxidation state, no further reduction is possible and, as will be discussed further below, this shift is assigned to electron transfer from cations in alumina to molybdenum.

Fig. 7c displays the C 1s spectral region as a function of annealing temperature. These data are in accord with the Auger results shown in Fig. 2 and TPD data shown in Fig. 3. Fig. 7d shows the corresponding O 1s region as a function of annealing temperatures, where from 700 to 1400 K, the O 1s binding energy changes gradually from 531 to 532 eV, increasing slightly in intensity and then decreasing drastically on heating to 1400 K.

Although the aluminum film is oxidized following Mo(CO)$_6$ adsorption at 700 K (Figs. 1 and 5), metallic aluminum is still found to desorb from the surface (Fig. 3). It may be that this aluminum diffuses from deep within the sample. In order to further explore this phenomenon, additional experiments were performed by depositing a thinner aluminum film (~1/10th the thickness of that used in previous experiments).

Fig. 8a reveals that the initially deposited, thinner aluminum film also has two Al oxidation states at 72.0 eV (metallic) and at 74.5 eV (Al^{3+}), identical to those found for the thicker film (Fig. 5a). In this case, the substrate Mo 3d features are clearly visible indicating that all of the thinner aluminum film is sampled by XPS. After reacting with 100 L of Mo(CO)$_6$ at 700 K, the metallic aluminum feature (Fig. 8a) essentially completely disappears and no further changes are noted following 300 and 500 L Mo(CO)$_6$ exposures indicating that the thinner aluminum film is completely oxidized. Fig. 8b shows the corresponding C 1s spectrum where graphite (284.4 eV BE) is found after aluminum deposition, consistent with the data shown in Fig. 5b. A carbide feature appears at 282.7 eV BE and grows with increasing Mo(CO)$_6$ exposure. Fig. 8c displays the corresponding O 1s features. Prior to Mo(CO)$_6$ exposure, an O 1s binding energy of 531.6 eV is found, typical of oxygen bound to aluminum [45]. With increasing Mo(CO)$_6$ exposure, the binding energy decreases slightly so that, for a Mo(CO)$_6$ exposure of 500 L, the feature shifts to 531.2 eV BE. This implies that some oxygen adsorbs on Mo sites [44]. The oxygen signal does not increase significantly in intensity for Mo(CO)$_6$ exposures larger than 100 L, implying that the thinner aluminum film has been completely oxidized at a Mo(CO)$_6$ exposure of 100 L. The corresponding Mo signal is not shown since it, in this case, contains a significant contribution from the Mo(1 0 0) substrate.

Fig. 9 displays the effect of annealing the thinner aluminum film that has been completely oxidized by exposure to 500 L of Mo(CO)$_6$. During annealing, the Al 2p binding en-
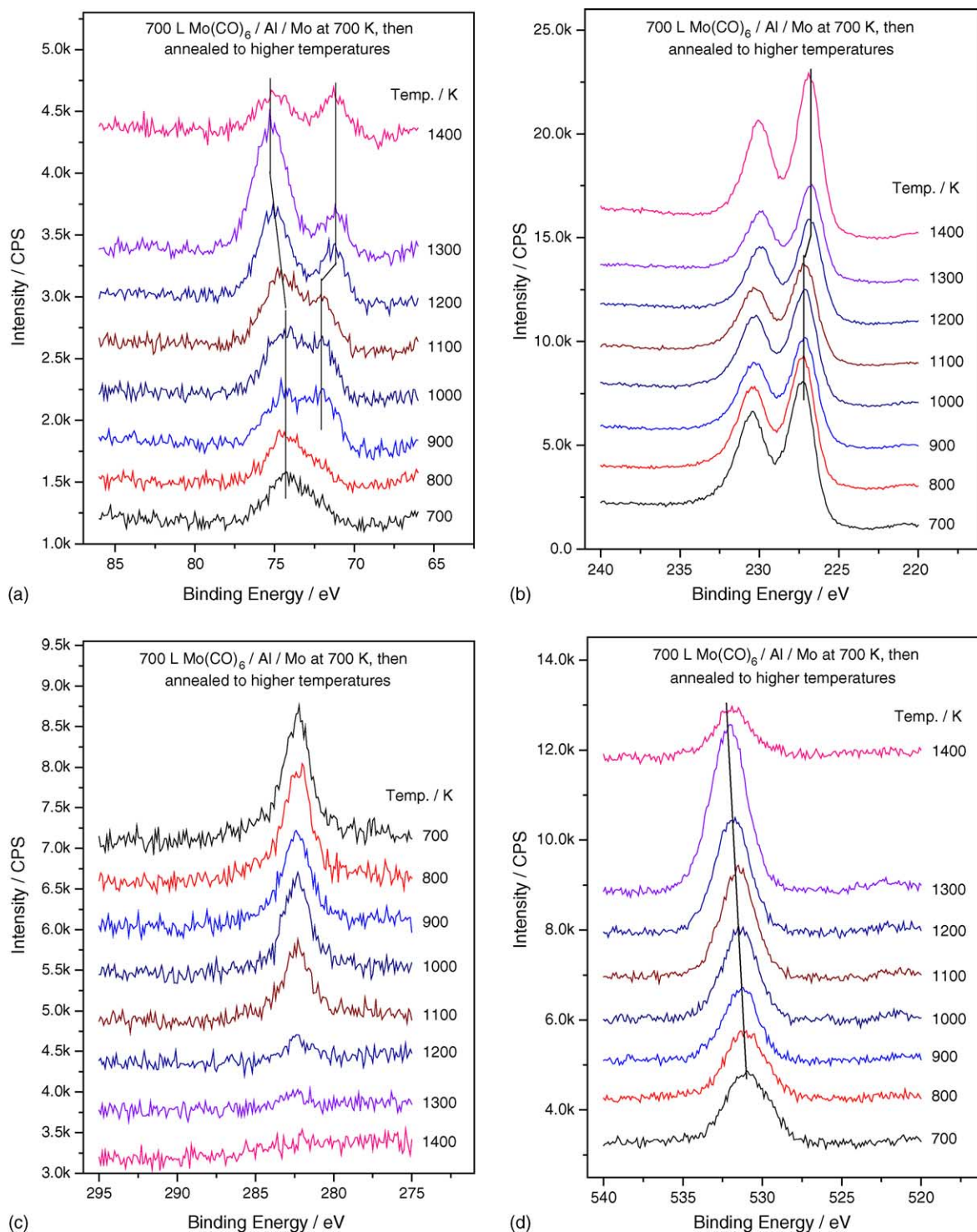
Fig. 7. Narrow scan Mg Kα X-ray photoelectron spectra of 700 L of Mo(CO)$_6$ deposited onto a thin aluminum film on Mo(1 0 0) at 700 K as a function of annealing temperature, where the annealing temperatures are marked adjacent to the corresponding spectra: (a) Al 2p, (b) C 1s, (c) Mo 3d and (d) O 1s regions.

ergy changes from 74.5 to 74.8 eV and is ascribed to alumina reduction by carbide as found for the thicker films (Fig. 7a). However, since only a small carbide signal is found (Fig. 8b), the reduction is not extensive. In addition, no metallic Al 2p signal at 72 eV is detected, indicating that alumina cannot be completely reduced by the surface carbide. Fig. 9b shows

the C 1s region as a function of annealing temperature where identical behavior is found as for the thicker aluminum film (Fig. 7c). Fig. 9c displays the corresponding O 1s regions where the binding energy increases from 531.3 to 531.6 eV suggesting that, during annealing, the small amount of oxygen bound to Mo species desorbs completely.
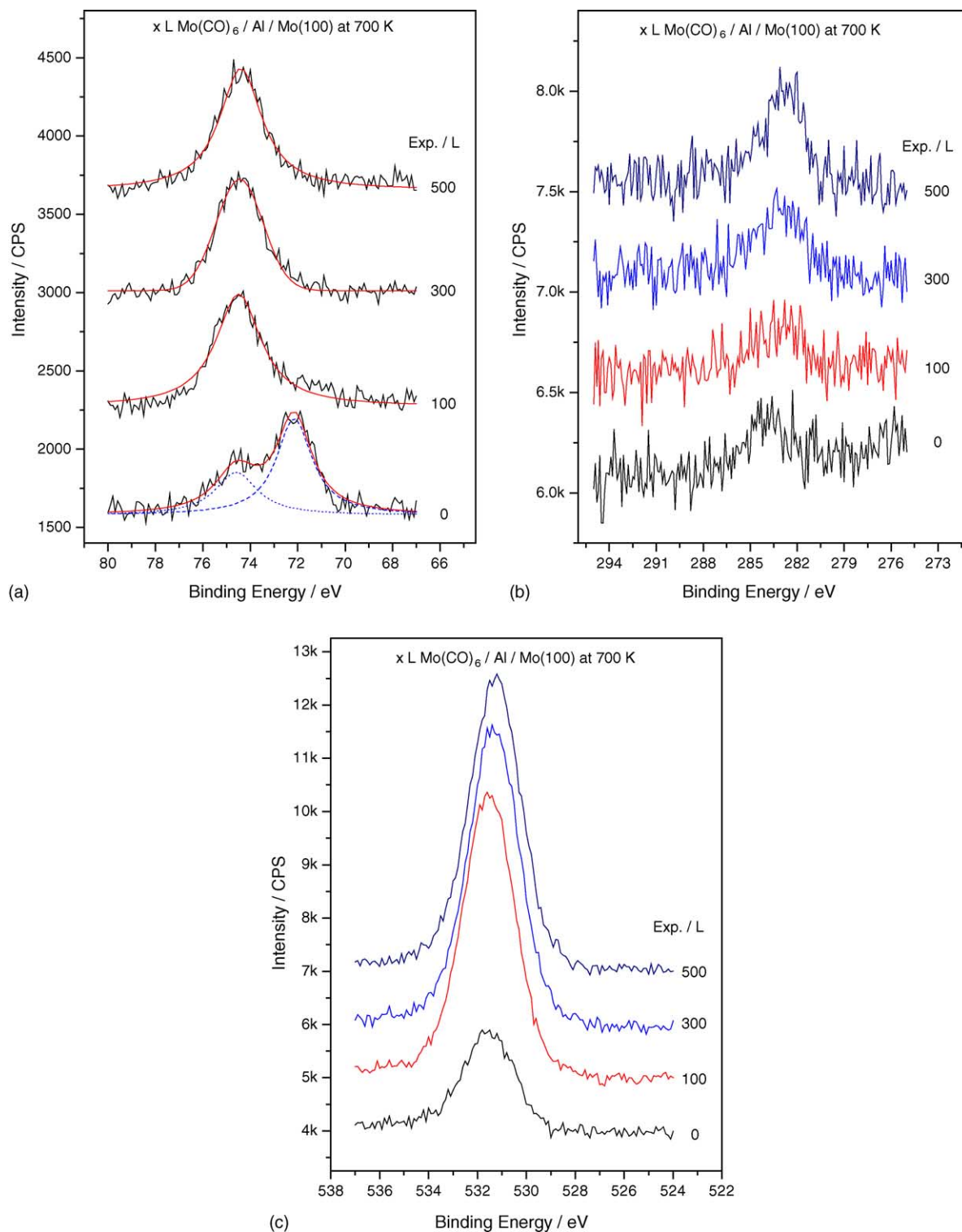
Fig. 8. Narrow scan Mg Kα X-ray photoelectron spectra of Mo(CO)$_6$ deposited onto a very thin aluminum film on Mo(1 0 0) at 700 K as a function of Mo(CO)$_6$ exposure, where the exposures are marked adjacent to the corresponding spectrum: (a) Al 2p, (b) C 1s and (c) O 1s regions.

The O 1s binding energy decrease during Mo(CO)$_6$ adsorption shown in Figs. 5d and 8d suggests some oxidation of the molybdenum [44]. However, no Mo binding energy greater than 227.4 eV (corresponding to metallic molybdenum) is observed. This indicates that molybdenum is only slightly oxidized during Mo(CO)$_6$ adsorption. Molybdenum has four prominent Auger transitions at 119, 160, 186 and 221 eV, with the 186 eV feature being
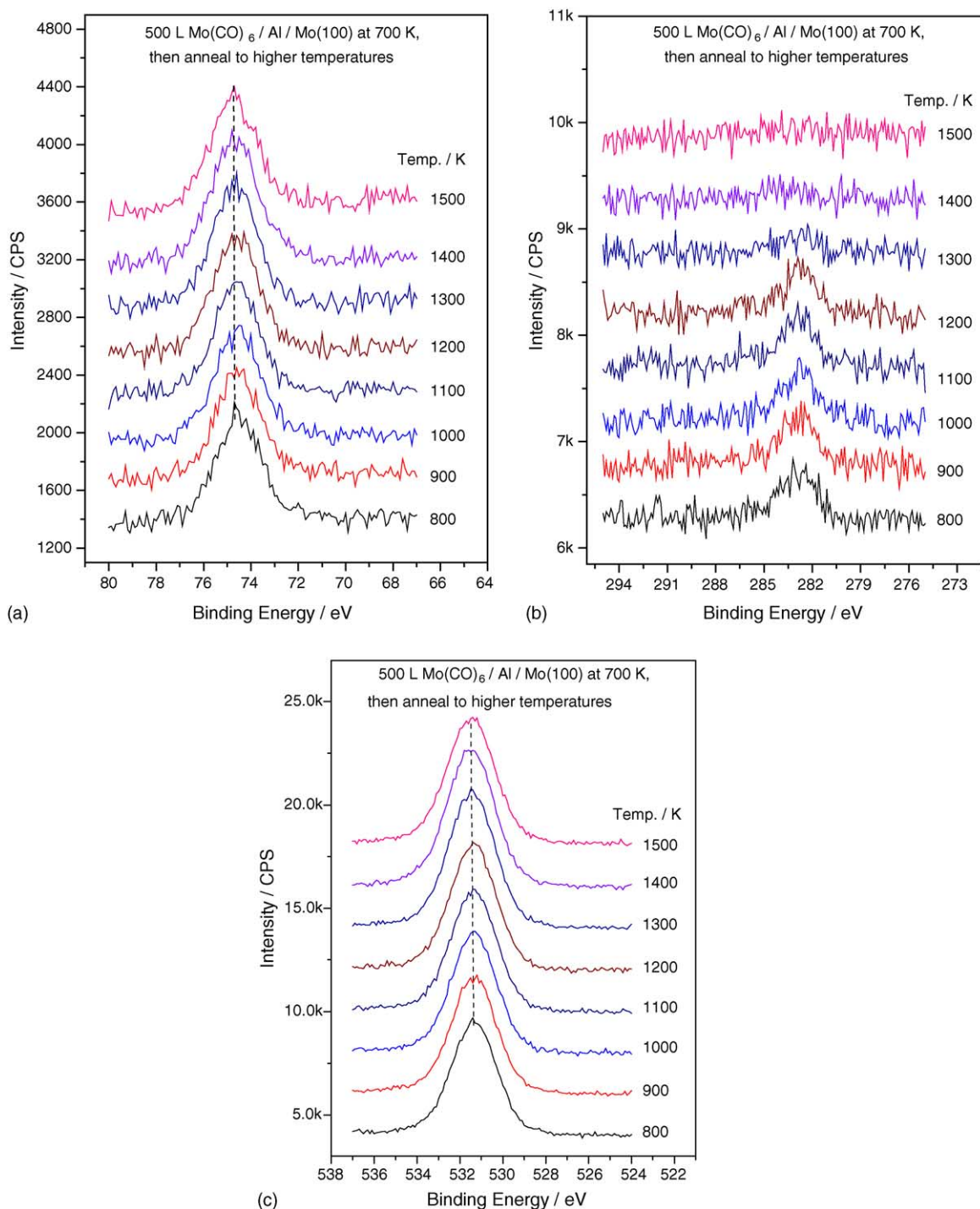
Fig. 9. Narrow scan Mg Kα X-ray photoelectron spectra of 500 L of Mo(CO)$_6$ deposited onto a very thin aluminum film on Mo(1 0 0) at 700 K as a function of annealing temperature, where the annealing temperatures are marked adjacent to the corresponding spectra: (a) Al 2p, (b) C 1s and (c) O 1s regions.

the most intense. Wolowik and Janik-Czachor [46] found that the peak-to-peak intensity ratios of these transitions change when molybdenum is oxidized. For pure Mo, the ratio $I_{119\,eV}/I_{186\,eV} = 0.19$, $I_{160\,eV}/I_{186\,eV} = 0.37$, and $I_{221\,eV}/I_{186\,eV} = 0.88$ where these values are measured for the clean Mo(1 0 0) substrate. If molybdenum is oxidized, the ratios $I_{119\,eV}/I_{186\,eV}$ and $I_{160\,eV}/I_{186\,eV}$ are expected to increase

and the ratio $I_{221\,eV}/I_{186\,eV}$ to decrease. Fig. 10a plots these ratios measured from the data in Fig. 1a and b as a function of Mo(CO)$_6$ exposure. Evidently, for low Mo(CO)$_6$ exposures, molybdenum is metallic presumably since oxygen mainly adsorbs on aluminum. For Mo(CO)$_6$ exposures of 75 L or higher, it is evident that molybdenum oxidizes slightly. Fig. 10b plots these ratios as a function of annealing tem-
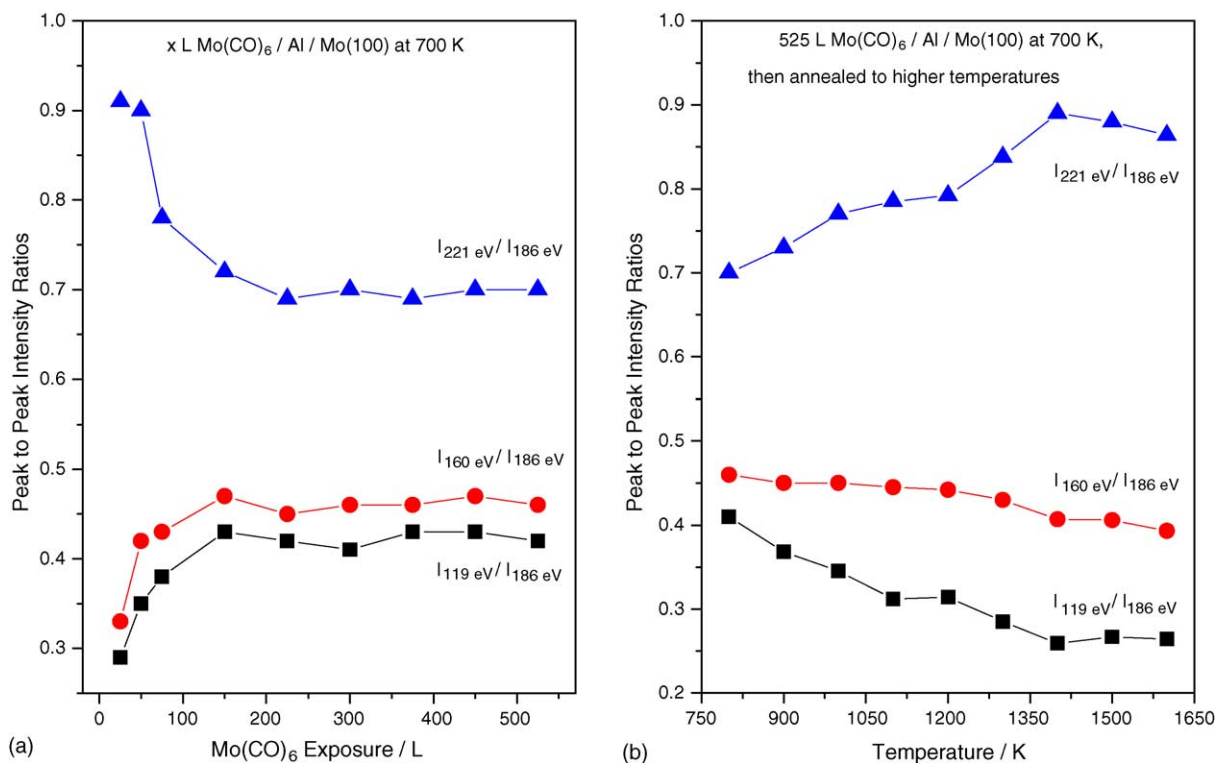
Fig. 10. Peak-to-peak Auger intensity ratios of deposited Mo: (a) as a function of $Mo(CO)_6$ exposure at 700 K and (b) as a function of annealing temperature.

perature indicating that molybdenum is reduced on heating so that, by ~1400 K, only metallic molybdenum is present.

4. Discussion

4.1. Nature of the film grown at 700 K

We focus initially on the nature of the film formed by $Mo(CO)_6$ adsorption on the aluminum film at 700 K. When $Mo(CO)_6$ is adsorbed at lower temperatures (~200 K), the majority of the carbonyl desorbs molecularly with a small proportion adsorbing strongly on the surface to evolve predominantly CO in temperature-programmed desorption, where all the CO has desorbed by 600 K [28–31]. It is therefore possible to deposit pure molybdenum if CO adsorption can be completely eliminated. Metallic molybdenum adsorption has been achieved by Biener and Friend [47] using a gold substrate and low $Mo(CO)_6$ exposures. CO disproportionation has also been proposed as a route by which carbon is deposited onto the surface [48].

Because of its reactivity, it is difficult to deposit pure aluminum on the surface in spite of the low background pressure during these experiments and extensive initial outgassing of the evaporation source. The initial film therefore contains a very small amount of carbon, both in the form of carbide (~281 eV BE, Fig. 5b) and graphite (284.5 eV, Figs. 5b and 8b). Both XPS (Figs. 5d and 8c) and Auger spectroscopy (Fig. 1a) reveal the presence of oxygen on the surface, which results in a portion of the surface region of aluminum being present as Al^{3+} (Figs. 5a and 8a).

The data of Fig. 4b indicate that the initial rate of molybdenum uptake is slower than that when molybdenum has been deposited onto the surface indicating that aluminum is less reactive for $Mo(CO)_6$ decomposition than the molybdenum carbonyl derived film. This transition occurs at a $Mo(CO)_6$ exposure of ~50 L suggesting that the aluminum surface becomes completely covered by the molybdenum-derived film at this exposure. The intensity of the XPS signal of the film should saturate at ~4λ, where λ is the mean free path of the electrons. In the case of molybdenum, this is ~10 Å [42] suggesting that a film of ~40 Å thick has been deposited at a $Mo(CO)_6$ dose of 500 L.

As the $Mo(CO)_6$ reacts with the surface at 700 K, the aluminum (Figs. 1a, 5a and 8a) and oxygen (Figs. 5d and 8c) signals decrease in intensity, while those for molybdenum and carbon (Figs. 1b and 5c) increase. This implies that the molybdenum is predominantly present as carbide. The atomic ratio of Mo and C is estimated from the intensities of Mo $3d_{5/2}$ and C 1s signals using the atomic sensitivity factors of Mo (1.75) and C (0.25) [49]. For a $Mo(CO)_6$ exposure of 50 L, when the surface just appears to be saturated, the calculated Mo/C ratio is ~1.1, suggesting MoC is formed in this case. When the exposure increases to 700 L, a Mo/C ratio of ~1.65 is obtained, indicating the carbide formed is closer to Mo_2C. This is an approximate estimate since the atomic sensitivity factors were obtained using electron analyzers operating in retarding mode while the analyzer in this work operated at
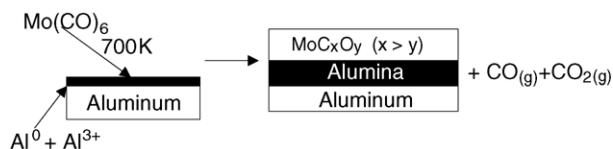
Scheme 1.

a constant pass energy. Using the AES data shown in Fig. 1 and the corresponding Auger sensitive factors [42], similar Mo/C ratios are obtained. This observation is in accord with the C 1s binding energy of 282.2 eV (Fig. 5b) and the shape of the C KLL Auger transition (Fig. 1b), which is indicative of carbide [29]. Apparently the formation of carbidic carbon is accompanied by aluminum oxidation by dissociated CO, where oxygen adsorbs onto aluminum and carbon bonds to molybdenum to form the carbide. Carbide formation could also be due partly to CO disproportionation [48]. If carbon were to originate entirely from this reaction, pure carbide would form. It is evident from the XPS data (Fig. 5d), however, that even the thickest carbonyl-derived films contain a small amount of oxygen and, as noted above, the O 1s binding energies indicate that the oxygen is associated with molybdenum implying the formation of an oxycarbide containing a relatively small amount of oxygen. Bugyi and Solymosi et al. [50] have studied the adsorption of CO on Mo_2C and found out that CO dissociates at 300–350 K and recombinative desorption occurs at 960 and 1060 K. The results shown in this work is consistent with their results; even if pure carbide were formed in the first place, it would eventually convert to an oxycarbide. Since it is difficult to precisely determine the amount of oxygen bound to aluminum compared to that bound to molybdenum, the stoichiometry of the oxycarbide is uncertain. The upper limit is MoCO where the C:O ratio is unity [51]. If MoCO is formed (where the Mo oxidation state is +2), a Mo 3d binding energy increase will be expected, but this is not observed (Fig. 5), suggesting that the O:C ratio in the oxycarbide is smaller than unity. The reaction chemistry at 700 K is summarized in Scheme 1.

4.2. Effect of annealing on the deposited film

We turn now to the effect of heating the initially deposited molybdenum (oxy)carbide film. As shown in Figs. 2a and 7a, intense aluminum Auger and XPS signals appear when the sample is heated to 900 K. This could arise either by reduction of alumina by carbidic carbon or the diffusion of metallic aluminum from deep within the film. It has been shown previously that alumina can be reduced by a carbide by growing the alumina film using $H_2^{18}O$ and detecting $C^{18}O$ in TPD following $Mo(CO)_6$ adsorption [29]. However, as indicated by the data shown in Fig. 3, only a small amount of CO desorbs at 900 K and the data of Fig. 2a show that, between 800 and 900 K, the Mo/C ratio does not change. This suggests that the increase in aluminum signal observed on heating to 900 K may be due to the diffusion of metallic aluminum from

within the film. TPD results (Fig. 3) reveal that a portion of the metallic Al desorbs from the surface between 1200 and 1350 K, with a maximum at 1260 K.

In order to further address this question, experiments were carried out on aluminum films that are sufficiently thin to be fully oxidized (Fig. 8). As this film is annealed (Fig. 9), no metallic aluminum (which would appear at ∼72 eV BE) is observed. However, the Al 2p BE shifts slightly from 74.5 to 74.8 eV. Note that a similar change in binding energy is also observed in Fig. 7a, where the 74.5 eV BE feature shifts to 75.4 eV upon annealing. It has been found previously [52] that annealing sapphire to 1400 °C desorbs oxygen from the top two layers, leaving an aluminum rich surface where a ∼2 eV Al 2p BE increase was found with XPS in that case and the shift noted in Figs. 7a and 9a are ascribed to a similar effect. Note that this is in accord with the reduction in the C 1s signal intensity on annealing (Figs. 7c and 9b), and the desorption of CO (Fig. 3). This reduction, however, is not extensive since no 72 eV signal is observed in Fig. 9. Following the above arguments, it is therefore proposed that the aluminum signal (72 eV BE) appearing at 900 K (Figs. 2a and 7a), as well as the desorbing aluminum (Fig. 3), are due to metallic aluminum diffusing from the bulk of the film, while the increase in binding energy (to 75.4 eV, Fig. 7a) is assigned to alumina reduction.

On heating to higher temperatures, above ∼1200 K, both the aluminum and molybdenum signals decrease in binding energy, implying some interaction between the aluminum and molybdenum. The formation of a molybdate can be immediately excluded since this would yield a Mo $3d_{5/2}$ feature at ∼233.6 eV BE [42], while no features are observed at this energy. An alternative possibility is the formation of a MoAl alloy. There are several points to support this argument. In general, molybdenum has a very low solubility in aluminum and it is not used as an alloying element for aluminum. However, molybdenum concentrations of up to 55 at.% can be attained if the alloys are prepared using non-equilibrium methods, such as ion implantation or vapor or sputter deposition [53]. Blank experiments were carried out to deposit aluminum directly onto the Mo(1 0 0) surface. It is found that adsorbed aluminum desorbs completely at ∼1280 K, while metallic aluminum is still detectable at 1400 K (Fig. 7a) and 1600 K (Fig. 2a) after molybdenum deposition from $Mo(CO)_6$. This suggests the possibility that the presence of the film on top of the slightly oxidized aluminum film retains the aluminum on the surface at higher temperatures allowing it to alloy with the aluminum.

However, it has been found previously that forming alloys between aluminum and other transition metals (Ni, Pd) causes a decrease in Al binding energy, but an increase in transition metal binding energy. One would expect electron transfer from the less electronegative aluminum (pauling electronegativity, $E_P = 1.61$) to the more electronegative transition metal ($E_P(Ni) = 1.91$, $E_P(Pd) = 2.2$) leading to the opposite shift in binding energy to that found experimentally. This contradiction has been rationalized by proposing that the transition

metals (Ni and Pd) gain d-electrons, but lose sp-electrons, where the second effect outweighs the first leading to a net electron loss [54,55]. This effect does not explain the decrease in binding energy for molybdenum (Fig. 7b). However, it has found in systems in which a metal is deposited onto an alumina layer grown on aluminum, for example, $Ni/Al_2O_3/Al$ and $Pd/Al_2O_3/Al$, that electron transfer from the cations on the oxide surface to the transition metal clusters causes a binding energy decrease of the transition metals [56,57]. A similar effect may occur in the case of the proposed MoAl alloy in this case.

5. Conclusions

Molybdenum hexacarbonyl initially reacts with an aluminum film deposited onto a Mo(1 0 0) single crystal in ultrahigh vacuum at 700 K to form molybdenum (oxy)carbide on a thin alumina layer formed on the aluminum substrate. The carbonyl reacts immediately on the aluminum surface to form MoC, while subsequent layers produce Mo_2C. In addition, a small amount of oxygen is incorporated into the carbide. Heating this layer evolves predominantly carbon monoxide due to a reaction between the molybdenum carbide and oxidized aluminum. Aluminum diffuses from the metal layer below, some of which desorbs at ~1300 K, the remainder being retained on the surface and it is proposed that the aluminum retained on the surface at this temperature forms an alloy with molybdenum.

Acknowledgment

References

[1] A. Brenner, J. Mol. Catal. 5 (1979) 157.
[2] E. Davie, D.A. Whan, C. Kemball, J. Catal. 24 (1972) 272.
[3] J. Smith, R.F. Howe, D.A. Whan, J. Catal. 34 (1974) 191.
[4] R. Thomas, J.A. Moulijn, J. Mol. Catal. 15 (1982) 157.
[5] A. Brenner, R.L. Burwell Jr., J. Am. Chem. Soc. 97 (1975) 2565.
[6] A. Brenner, R.L. Burwell Jr., J. Catal. 52 (1978) 353.
[7] R.F. Howe, Inorg. Chem. 15 (1976) 486.
[8] A. Kazusaka, R.F. Howe, J. Mol. Catal. 9 (1980) 183.
[9] K.P. Reddy, T.L. Brown, J. Am. Chem. Soc. 117 (1995) 2845.
[10] A. Zecchina, E.E. Platero, C.O. Areán, Inorg. Chem. 27 (1988) 102.
[11] R.F. Howe, I.R. Leith, J. Chem. Soc., Faraday Trans. I 69 (1973) 1967.
[12] W.M. Shirley, B.R. McGarvey, B. Maiti, A. Brenner, A. Cichowlas, J. Mol. Catal. 29 (1985) 259.
[13] J. Libuda, M. Frank, A. Sandell, S. Andersson, P.A. Bruhwiler, M. Baumer, N. Martensson, H.-J. Freund, Surf. Sci. 384 (1997) 106.
[14] B. Domenichini, A.M. Flank, P. Lagarde, S. Bourgeois, Surf. Sci. 560 (2004) 63.
[15] X. Zhao, J. Hrbek, J.A. Rodriguez, Surf. Sci. 575 (2005) 115.
[16] K. Okumura, S. Huodo, S. Noda, J. Phys. Chem. B 105 (2001) 8345.
[17] P.J. Chen, D.W. Goodman, Surf. Sci. 312 (1994) 767.
[18] H.H. Madden, D.W. Goodman, Surf. Sci. 150 (1985) 39.
[19] P.J. Chen, D.W. Goodman, J.T. Yates Jr., Phys. Rev. B 41 (1990) 8025.
[20] B.G. Frederick, G. Apai, T.N. Rhodin, Surf. Sci. 244 (1991) 67.
[21] T.N. Rhodin, B.G. Frederick, G. Apai, Surf. Sci. 287 (1993) 638.
[22] C. Brüesch, R. Kötz, N. Neff, L. Pietronero, Phys. Rev. B 29 (1984) 4691.
[23] C. Xu, W.S. Oh, G. Liu, D.Y. Kim, D.W. Goodman, J. Vac. Sci. Technol. A 15 (1997) 1261.
[24] T.N. Rhodin, R.P. Merril, P.J. O'Hagan, S.C. Woronick, N.D. Shinn, G.L. Woolery, A.W. Chester, J. Phys. Chem. 98 (1994) 2433.
[25] B.G. Frederick, G. Apai, T.N. Rhodin, Surf. Sci. 277 (1992) 337.
[26] A.J. Maeland, R. Rittenhause, W. Lahar, P.V. Romano, Thin Solid Films 21 (1974) 67.
[27] F.P. Mertens, Surf. Sci. 71 (1978) 161.
[28] M. Kaltchev, W.T. Tysoe, J. Catal. 193 (2000) 29.
[29] M. Kaltchev, W.T. Tysoe, J. Catal. 196 (2000) 40.
[30] Y. Wang, F. Gao, M. Kaltchev, D. Stacchiola, W.T. Tysoe, Catal. Lett. 91 (2003) 88.
[31] Y. Wang, F. Gao, M. Kaltchev, W.T. Tysoe, J. Mol. Catal. A: Chem. 209 (2004) 135.
[32] Z. Jiang, W. Huang, J. Jiao, H. Zhao, D. Tan, R. Zhai, X. Bao, Appl. Surf. Sci. 229 (2004) 43.
[33] P. Liu, J.A. Rodriguez, J.T. Muckerman, J. Hrbek, Surf. Sci. 530 (2003) 313.
[34] C.C. Williams, J.G. Ekerdt, J. Phys. Chem. 97 (1993) 6843.
[35] L. Rodrigo, K. Marcinkowska, P.C. Roberge, S. Kaliaguine, J. Catal. 107 (1987) 8.
[36] I.V. Elav, B.N. Shelimov, V.B. Kazansky, J. Catal. 113 (1988) 256.
[37] M. Kurhinen, S. Myllyoja, M. Suvanto, T.A. Pakkanen, J. Mol. Catal. A: Chem. 154 (2000) 229.
[38] R.I. Nakamura, R.G. Bowman, R.L. Burwell, J. Am. Chem. Soc. 103 (1981) 673.
[39] M.G. Kaltchev, A. Thompson, W.T. Tysoe, Surf. Sci. 391 (1997) 145.
[40] W.J. Wytenburg, R.M. Lambert, J. Vac. Sci. Technol. A 10 (1992) 3597.
[41] D. Briggs, M.P. Seah, Practical Surface Analysis Auger and X-ray Photoelectron Spectroscopy, Wiley, 2004.
[42] D. Briggs, J.T. Grant, Surface Analysis by Auger and X-ray Photoelectron Spectroscopy, IM Publications and Surface Spectra Limited, UK, 2003.
[43] K. Edamoto, M. Sugihara, K. Ozawa, S. Otani, Appl. Surf. Sci. 237 (2004) 498.
[44] T. Schroeder, J. Zegenhagen, N. Magg, B. Immaraporn, H.-J. Freund, Surf. Sci. 552 (2004) 85.
[45] B.R. Strohmeier, Surf. Sci. Spectra 3 (1995) 135.
[46] A. Wolowik, M. Janik-Czachor, Mater. Sci. Eng. A267 (1999) 301.
[47] M.M. Biener, C.M. Friend, Surf. Sci. Lett. 559 (2004) 173.
[48] G. Henrici-Olive, S. Olive, The Chemistry of the Catalyzed Hydrogenation of Carbon Monoxide, Springer-Verlag, Berlin, 1984.
[49] C.D. Wagner, L.E. Davis, M.V. Zeller, J.A. Taylor, R.M. Raymond, L.H. Gale, Surf. Interf. Anal. 3 (1981) 211.
[50] L. Bugyi, F. Solymosi, J. Phys. Chem. B 105 (2001) 4337.
[51] X. Li, Y. Li, Chem. Eur. J. 10 (2004) 433.
[52] M. Gautier, J.P. Duraud, L. Pham Van, M.J. Guittet, Surf. Sci. 250 (1991) 71.
[53] M. Janik-Czachor, A. Wolowik, A. Szummer, K. Lublinska, S. Hofmann, K. Kraus, Electrochim. Acta 43 (1998) 875.
[54] N.R. Shivaparan, V. Shutthanandan, V. Krasemann, R.J. Smith, Surf. Sci. 373 (1997) 221.
[55] V. Shutthanandan, A.A. Saleh, R.J. Smith, Surf. Sci. 450 (2000) 204.
[56] J.A. Horsley, J. Am. Chem. Soc. 101 (1979) 2870.
[57] T.J. Sarapatka, Chem. Phys. Lett. 212 (1993) 37.